Analyst

Efficient and rapid linker optimization with heterodimeric coiled coils improves the response of fluorescent biosensors comprising antibody and protein M

Journal:	*Analyst*
Manuscript ID	AN-COM-09-2023-001499.R1
Article Type:	Communication
Date Submitted by the Author:	20-Oct-2023
Complete List of Authors:	Sasamoto, Kana; Tokyo Institute of Technology School of Life Science and Technology Yasuda, Takanobu; Tokyo Institute of Technology, Zhu, Bo; Tokyo Institute of Technology IIR, Ueda, Hiroshi; Tokyo Institute of Technology, Laboratory for Chemistry and Life Science Kitaguchi, Tetsuya; Tokyo Institute of Technology, Laboratory for Chemistry and Life Science

SCHOLARONE™
Manuscripts

Please do not adjust margins

ARTICLE

Efficient and rapid linker optimization with heterodimeric coiled coils improves the response of fluorescent biosensors comprising antibody and protein M

Received 00th January 20xx,
Accepted 00th January 20xx

DOI: 10.1039/x0xx00000x

Kana Sasamoto,[a] Takanobu Yasuda,[b] Bo Zhu,[b] Hiroshi Ueda[b†] and Tetsuya Kitaguchi*[b]

We developed the coiled Q-probe (CQ-probe), a fluorescent probe containing the coiled-coil peptide pair E4/K4, to convert antibodies into biosensors for homogeneous immunoassays. This probe consists of an antibody-binding protein, protein M (PM) with the E4 peptide and the K4 peptide with a fluorescent dye. Compared to PM Q-probes, which are generated by modifying the C-terminus of PM with a fluorescent dye, CQ-probe variants with various linkers are easy to prepare and therefore enable the establishment of biosensors with a significant fluorescent response by localizing the fluorescent dye at the optimal position for quenching and antigen-dependent release. The fluorescence changes of biosensors converted from anti-BGP, anti-cortisol, and anti-testosterone antibodies using the rhodamine 6G (or TAMRA)-labeled CQ-probe upon antigen addition were 13 (or 2.6), 9.7 (or 1.5), and 2.1 (or 1.2) times larger than that of the biosensors converted using the PM Q-probe. Furthermore, the CQ-probe converted anti-digoxin IgG into a functional biosensor, whereas the PM Q-probe/antibody complex showed an insufficient response. This technology exhibits a promising capacity to convert antibodies into high-response biosensors, which are expected to be applied in a wide range of fields, including clinical diagnosis, environmental surveys, food analysis, and biological research.

Introduction

The PM Quenchprobe (PM Q-probe) is a protein M (PM)[1]-based fluorescent probe that converts an antibody or its fragment, Fab, into a biosensor by binding to the light chain of the antibody without gene manipulation of the antibody.[2] The operation principle of the PM Q-probe/antibody complex for antigen detection is homogeneous, and it does not require a washing step to remove antibodies, to which antigens are not bound. Moreover, because this technology can be applied to commercially available antibodies, it is a very promising immunoassay for the detection of myriad molecules.

The PM Q-probe is generated by modifying the C-terminus of protein M with a fluorescent dye, such as TAMRA. The C-terminally modified fluorescent dye of the PM Q-probe is quenched by tryptophan (Trp) residues in the antibody via photoinduced electron transfer (PET) when complexed with the antibody. When the antigen binds to the antibody, the fluorescent dye is released from the vicinity of the Trp residues and fluoresces. The range of K_D values between Trp and various fluorescent dyes is 4.9–130 mM (71 mM for TAMRA), and the interaction between Trp residues and the dye in PM Q-probe/antibody complex is likely to be stronger than the affinity from the K_D value because of higher local concentration derived from the tethered dye.[3] Since PM Q-probe/antibody complex showed fluorescence response, the interaction allows antigen binding followed by dye release.

Although the PM Q-probe was applied to several antibodies for conversion into biosensors, not all complexes showed a sufficient fluorescence response after the addition of the antigen. This weak response is thought to be due to differences in the position of the Trp residue in each antibody, meaning that, in some cases, the fluorescent dye was unable to localize to the optimized position for quenching and de-quenching before and after antigen binding, respectively. The fluorescence response of the Quenchbody (Q-body) which has a similar working principle to the PM Q-probe, has reportedly been improved by optimizing the linker between the antibody and the fluorescent dye.[4–8] Therefore, we considered that all antibodies could be converted into biosensors with a high response if the linker between the PM and the fluorescent dye was comprehensively optimized for each antibody.

Here, we aimed to improve the efficiency and speed of linker optimization by combining a PM with a coiled-coil-forming peptide pair, E4 and K4. E4/K4 is a peptide pair of $(EIAALEK)_4$ and $(KIAALKE)_4$, which was rationally designed to exhibit high affinity and specificity between them.[9] This unique property has been used for the fluorescent dye labeling of proteins such as cell surface receptors and antibodies without removing free dyes.[10-11]

[a]*Graduate School of Life Science and Technology, Tokyo Institute of Technology, 4259 Nagatsuta-cho, Midori-ku, Yokohama, Kanagawa 226-8503, Japan*
[b]*Laboratory for Chemistry and Life Science, Institute of Innovative Research, Tokyo Institute of Technology, 4259 Nagatsuta-cho, Midori-ku, Yokohama, Kanagawa 226-8503, Japan*
†*Deceased.*
Electronic Supplementary Information (ESI) available: [details of any supplementary information available should be included here]. See DOI: 10.1039/x0xx00000x

Please do not adjust margins

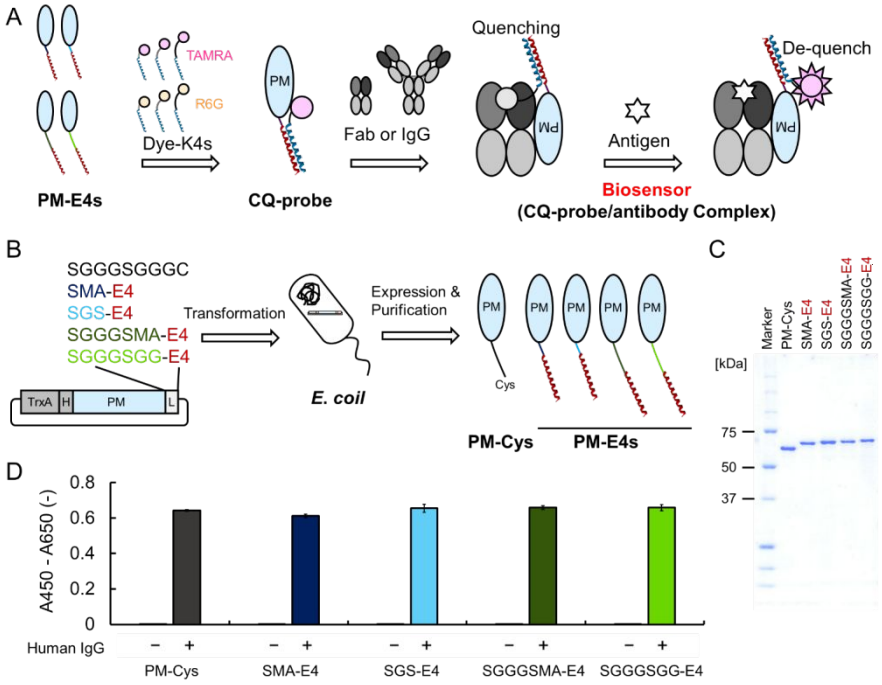

Fig. 1 Concept, design, and fabrication of the CQ-probe/antibody complex. (A) Concept of the Coiled Quenchprobe (CQ-probe). (B) Design of Protein M-E4s (PM-E4s) and Protein M-Cysteine (PM-Cys). TrxA: Thioredoxin A; H: His_6 tag; L: Linker-Cys or E4 $(EIAALEK)_4$. (C) SDS-PAGE analysis of purified PM-E4s and PM-Cys. Respective molecular mass of PMs: PM-Cys, 65 kDa; SMA-E4, 68 kDa; SGS-E4, 68 kDa; SGGGSMA-E4, 69 kDa; and SGGGSGG, 69 kDa. (D) Binding activity of PM-E4s and PM-Cys against human IgG by enzyme-linked immunosorbent assay. The data represent means ± standard deviation (n = 3).

In this study, we generated four PM variants containing different linker lengths and sequences between PM and E4-peptide (PM-E4s), and three K4 variants containing different linker lengths between fluorescent dyes and K4 (Dye-K4s) for comprehensive and rapid linker optimization (Fig. 1A). When a PM-E4 and Dye-K4 were mixed, the E4 and K4 formed a heterodimer, producing a fluorescent probe, named a Coiled Q-probe (CQ-probe). Thus, CQ-probes with different linker lengths and spatial arrangements were assembled. When using a CQ-probe, the biosensors that showed insufficient responses using the PM Q-probe were converted into biosensors with significant responses.

Because this technology facilitates the replacement of fluorescent dyes and the labeling of chemicals and drugs, it is expected not only to accelerate the improvement of biosensors but also to support stable detection by labeling with two different fluorescent dyes, the selection of suitable antibodies for biosensors from a large library, and the development of drug–PM/antibody complexes for clinical therapy beyond analytical chemistry.

Experimental

Materials

Escherichia coli strains XL-10 Gold (Agilent, Santa Clara, CA, USA) and SHuffle T7 Express lysY (New England Biolabs, Tokyo, Japan) were used for cloning and protein expression, respectively. Restriction enzymes and bovine serum albumin were purchased from New England Biolabs (Ipswich, MA, USA). Oligonucleotides were purchased from Eurofins Genomics (Tokyo, Japan) (Table S1). KOD-Plus-Neo was obtained from Toyobo Biochemicals (Osaka, Japan) and used for PCR. In-Fusion HD cloning kit and TALON metal affinity resin were purchased from Takara Bio (Shiga, Japan). The ImmunoBlock was purchased from KAC (Kyoto, Japan). Strep-Tactin-horseradish peroxidase conjugate was obtained from Bio-Rad (Hercules, CA, USA). 3,3’,5,5’-Tetramethylbenzidine (TMBZ) was purchased from Sigma-Aldrich (St. Louis, MO, USA). 5-TAMRA-C6 maleimide and ATTO-rhodamine 6G (R6G)-maleimide were obtained from AAT BioQuest (Sunnyvale, CA, USA) and ATTO-TEC (Siegen, Germany), respectively. Anti-testosterone (4E1G2) and anti-digoxin (HY-1A) monoclonal antibodies were obtained from Abnova (Taoyuan, Taiwan) and Jackson ImmunoResearch (West Grove, PA, USA), respectively. The peptides used in this study were purchased from LifeTein (Somerset, NJ, USA) (Table S2). Protein G Mag Sepharose Xtra was purchased from Cytiva (Tokyo, Japan). Testosterone and digoxin were purchased from Sigma-Aldrich and Tokyo Chemical Industry Co. Ltd. (Tokyo, Japan), respectively. Other chemicals and reagents were obtained from Wako Pure Chemicals (Osaka, Japan) unless otherwise noted. Ultrapure water was prepared using a Milli-Q system (Merck Millipore, Tokyo, Japan).

Construction of expression plasmids

The E4-2_Bottom (N-terminal) primer and each of the four Bsu_(Linker)_E4back (Linkers: SMA, SGS, SGGGSMA, SGGGSGG) primers were annealed to create the four N-terminal inserts, and E4-3_Top and_Eag_E4For_v2 were annealed to create the C-terminal insert (Table S1). The C-

 This journal is © The Royal Society of Chemistry 20xx

terminal insert and each of the four N-terminal inserts were introduced into the Bsu36I- and EagI-digested fragments of pET-TrxAHis2ST-PM-C[2] using the In-Fusion HD Cloning Kit, and four different pET-TrxAHis2ST-PM-(Linker)-E4 plasmids were constructed.

Protein production and purification

SHuffle T7 Express lysY cells were transformed with the pET-TrxAHis2ST-PM-C, pET-TrxAHis2ST-PM-(Linker)-E4, or pET-Fab (KTM219) plasmid,[12] and were cultured at 30 °C overnight on Luria–Bertani broth with ampicillin (100 μg/mL, LBA) plates (1.5% agar). A single colony was picked and cultivated in 4 mL LBA medium for 16–20 h at 30 °C. Four milliliters of culture were added to 400 mL of LBA and cultivated at 30 °C until OD600 reached 0.4–0.7. Isopropyl-β-thiogalactopyranoside was added to the culture medium (f.c. 0.4 mM) and the culture was shaken for 16–20 h at 16 °C, 200 rpm. The culture medium was centrifuged (8,000 g, 10 min, 4 °C) to obtain *E. coli* pellets. Each pellet was resuspended in 9 mL of phosphate buffer (20 mM phosphate, 0.5 M NaCl, pH 7.2), followed by lysate collection after *E. coli* disruption using a Cell Disrupter One Shot model (Constant Systems Ltd., Daventry, UK). The collected lysate was centrifuged (8,000 g, 10 min, 4 °C) and the supernatant was stirred with 200 μL (slurry volume) of TALON immobilized metal affinity chromatography resin on a vertical tube rotator for 1 h at 4 °C. After centrifugation (100 g, 1 min, 4 °C), the resin was applied to a TALON 2 mL Disposable Gravity Column (Takara Bio). The resin was washed three times with wash buffer (20 mM phosphate, 0.5 M NaCl, 33 mM imidazole, pH 7.2) and eluted with 200 μL of elution buffer (20 mM phosphate, 0.5 M NaCl, 500 mM imidazole, pH 7.2) after 5 min incubation at 4 °C. Finally, the eluate was applied to a pre-equilibrated G-25 Microspin column (Cytiva) with phosphate-buffered saline (PBS), and the column was centrifuged (735 g, 1 min, 4 °C) to remove imidazole to obtain proteins. The PMs and Fab obtained were confirmed by SDS-PAGE, analyzed using a WISE-6100 LuminoGraph 1 (ATTO, Tokyo, Japan), and quantified using a standard curve prepared with bovine serum albumin.

Enzyme-linked immunosorbent assay

Normal Human IgG, Whole Molecule, Purified (Wako; 10 μg/mL), in PBS, were immobilized on a 96-well clear flat-bottomed polystyrene high-bind microplate (Costar3590, Corning-Costar Japan, Tokyo, Japan) overnight at 4 °C. The plate was then blocked using 20% ImmunoBlock in PBS with Tween 20 (0.1%) (PBST) at 25 °C for 2 h. After washing three times with PBST, PM (1 μg/mL) in PBST containing 5% ImmunoBlock was added to the well and incubated for 1 h at 25 °C. After washing three times with PBST, 3000 × diluted Strep-Tactin-horseradish peroxidase in PBST containing 5% ImmunoBlock was added to the well and incubated for 1 h at 25 °C. The wells were then washed thrice with PBST and 100 μL of substrate solution (100 μg/mL TMBZ and 0.03% hydrogen peroxide in 100 mM sodium acetate, pH 6.0) was added. After 2 min, 10% H_2SO_4 was added to stop the reaction, and the absorbance was measured at 450 nm using a microplate reader (SH-1000Lab, Corona Electric, Ibaraki, Japan) with 650 nm as the reference wavelength.

Fluorescent dye modification of the K4 peptide

K4 peptides with an N-terminal cysteine residue (45 nmol) and fluorescent dye-maleimide (10 nmol) were dissolved in 300 μL of PBS and stirred using a rotating mixer (CM-1000, EYELA, Japan) at 2,000 rpm in the dark for 2 h at 25 °C. The modified K4 peptides were purified using an HPLC system (Chromaster, Hitachi, Tokyo, Japan) with a C_{18} column (COSMOSIL 5C18-AR-II; 5 μm, 4.6 I.D. × 250 mm; Nacalai Tesque, Kyoto, Japan). Linear gradient elution was conducted using mobile phases A (H_2O with 0.1% (v/v) trifluoroacetic acid) and B (acetonitrile with 0.1% (v/v) trifluoroacetic acid) from 95:5 to 45:55 for 100 min at a flow rate of 1 mL/min. The molecular masses of the purified peptides were identified using matrix-assisted laser desorption/ionization-time of flight mass spectrometry (ultrafleXtreme, Bruker, MA, USA).

Preparation of CQ-probe/antibody complex and reaction with antigen

To obtain the CQ-probes, PM-E4s (50 nM) and Dye-K4s (30 nM) were mixed in PBST and incubated at 25 °C for 30 min in the dark. The CQ-probes were diluted to 1 nM and mixed with antibodies or antibody fragments (5–50 nM) in PBST. The mixture (337 μL) was incubated at 25 °C for 2 h 30 min in the dark to obtain the CQ-probe/antibody complex. Antigens (3 μL) at different concentrations were added to this complex and incubated at 25 °C for 30 min in the dark before fluorescence measurement.

Fluorescence measurement

Samples (100 μL/well) were added to a 96-well half-area black microplate (675076, Greiner Japan, Tokyo), and the fluorescence intensity was measured using a fluorescence microplate reader (Clariostar, BMG Labtech Japan, Saitama, Japan). The excitation and emission wavelengths were configured at 535/20 and 585/30 nm, and 515/20 and 570/30 nm for the TAMRA-K4 and R6G-K4 labeled CQ-probes, respectively (center wavelength/bandwidth). The dose-response curve was fitted to a four-parameter logistic equation (Eq. 1) using KaleidaGraph™ 5.0 (https://www.hulinks.co.jp/software/stat_graph/kaleida). The lower asymptote (A) was fixed at 1, and the value of C was estimated as the EC_{50}. The B is the hill coefficient and D is the normalized maximum asymptote. The limit of detection (LOD) was calculated as the concentration corresponding to the mean of the blank plus three times the standard deviation. The EC_{50} and LOD were calculated only when the coefficient of determination R^2 exceeded 0.96.

$$y = D + \frac{A - D}{1 + \left(\frac{x}{C}\right)^B} \quad (1)$$

Purification of anti-cortisol IgG from hybridoma supernatant

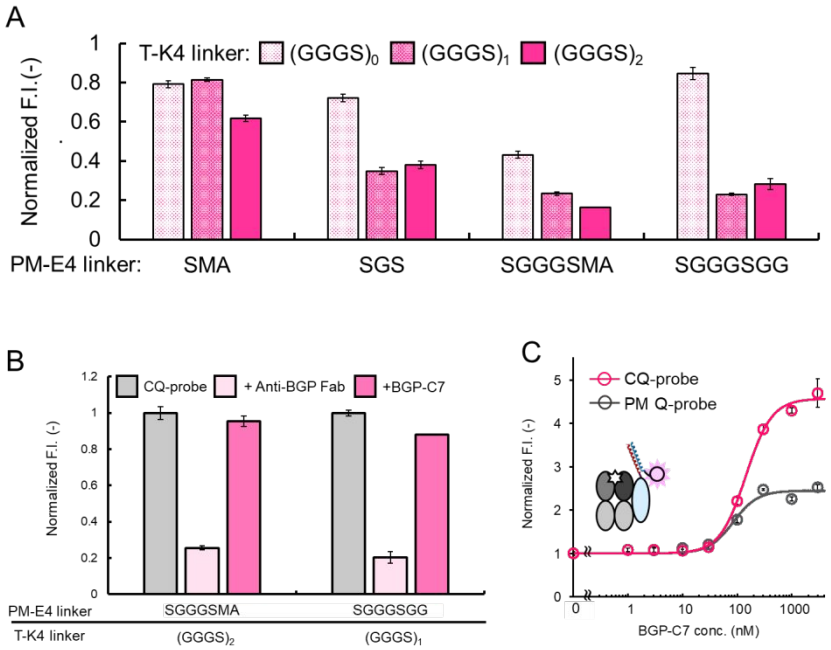

Fig. 2 Quenching and fluorescence response of CQ-probe/Fab complex. (A) Quenching level of 12 combinations of CQ-probe with different linkers (1.0 nM) mixed with the Fab fragment of KTM219 (50 nM). (B) Fluorescence response of selected CQ-probe (1.0 nM)/Fab (30 nM) complexes against the antigen BGP-C7 (3.0 μM). (C) Dose–response curves for CQ-probe (1.0 nM)/Fab (30 nM) and PM Q-probe (1.0 nM)/Fab (30 nM) complexes against BGP-C7. The linker combinations are the PM-E4 linker for SGGGSGG and the TAMRA-K4 (T-K4) linker for $(GGGS)_1$. The data represent means ± standard deviation (n = 3)

Anti-cortisol (CS) IgG (CS4-6)[13] was purified from the hybridoma culture supernatant using Protein G Mag Sepharose Xtra, according to the manufacturer's instructions.

Results and discussion

Preparation of PM-E4s and PM-cysteine

To search for the optimized linker between the PM and E4-peptide, we constructed PM-E4s containing linkers of different lengths and sequences (Fig. 1B). In a previous report, membrane proteins fused with E peptide were labeled with dye-K peptide, whereas K peptide fused membrane protein failed to be labeled by dye-E peptide, thus the PM was fused with E4 instead of K4.[10] The properties of the PM-E4 linkers were as follows: SMA was relatively short; SGS was more flexible than SMA; SGGGSMA was relatively long; and SGGGSGG was a flexible version of SGGGSMA. As a control, we utilized PM with a cysteine tag (PM-Cys), which is the unmodified protein with fluorescent dye for making PM Q-probe. When the PM-E4s and PM-Cys were expressed in *E. coli* and purified using a His_6 tag, SDS-PAGE analysis revealed single bands in all PMs, which approximately matched the expected molecular weight (Fig. 1C). To examine whether all PMs maintained antibody-binding activity after the C-terminal fusion of linkers with E4s, we performed an enzyme-linked immunosorbent assay against immobilized human polyclonal IgG. The absorbance signals of all PM-E4 variants were comparable to those of the control PM-Cys (Fig. 1D), suggesting that PM-E4s bind to antibodies with a similar affinity to that of PM-Cys. Therefore, the CQ-probe/antibody complex is expected to function as a biosensor, similar to the PM Q-probe/antibody complex.

Selection of optimized linkers for CQ-probes

Because PM Q-probe/antibody complexes with high fluorescence responses to antigen binding tend to also show high quenching levels,[2] we first examined the quenching levels of the 12 CQ-probe combinations using a model antibody. These 12 combinations, derived from the four linker variants of PM-E4 and three linker variants of TAMRA-K4 (T-K4) (Fig. S1A), were mixed with the Fab fragment of the anti-human osteocalcin (Bone Gla Protein, BGP) antibody KTM219 (Fig. S2A).[14] This Fab fragment was employed as a model antibody because it was utilized for the development of the Q-body via fluorescence modification in the N-terminal region.[11,15] The fluorescent dye TAMRA was employed because it is also commonly used in the Q-body and shows a significant PET-based quenching effect.[4,7,11]

We found that the fluorescence intensity of complexes with long PM-E4 linkers and T-K4 with $(GGGS)_1$ (or more repeats) was particularly reduced (Fig. 2A and Table S3A). We selected the two combinations with the deepest quenching levels and examined their fluorescence responses after the addition of the antigen. When the antigen peptide BGP-C7, NH_2-RRFYGPV-COOH, was added to the CQ-probe/Fab complexes, the PM-SGGGSGG-E4 and T-GGGS-K4 combinations resulted in strong fluorescence responses (Fig. 2B and Table S4A), which increased in a dose-dependent manner (Fig. 2C). The maximum response, fluorescence change, and LOD of the CQ-probe/Fab complexes were 4.6-fold, 360%, and 18 nM, respectively; the fluorescence response and LOD were

 This journal is © The Royal Society of Chemistry 20xx

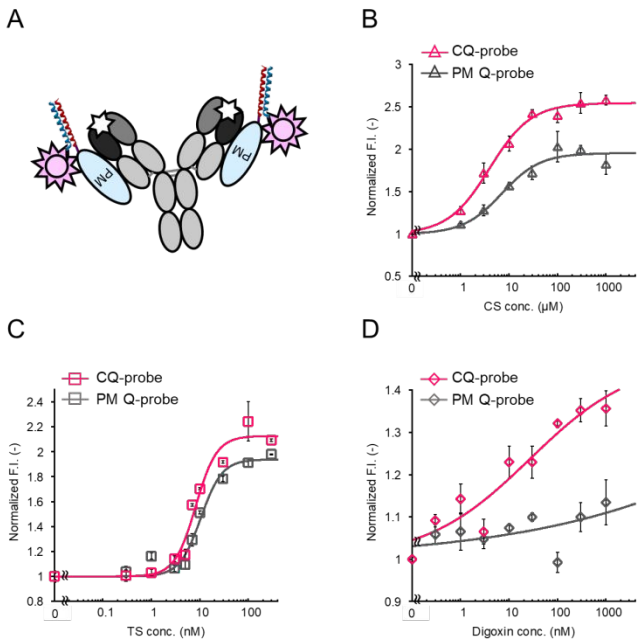

Fig. 3 Dose–response curve of T-K4 labeled CQ-probe/anti-hapten IgG complex against antigens. (A) Diagram of antigen detection by CQ-probe/IgG complex. (B) CQ-probe (1.0 nM)/IgG (5.0 nM) and PM Q-probe (1.0 nM)/IgG (5.0 nM) complexes against cortisol. The linker combinations were the PM-E4 linker for SGGGSMA and the T-K4 linker for $(GGGS)_0$. (C) CQ-probe (1.0 nM)/IgG (5.0 nM) and PM Q-probe (1.0 nM)/IgG (5.0 nM) complexes against testosterone. Linker combinations: PM-E4 linker for SGGGSMA and T-K4 linker for $(GGGS)_1$. (D) CQ-probe (1.0 nM)/IgG (10 nM) and PM Q-probe (1.0 nM)/IgG (10 nM) complexes against digoxin. Linker combinations: PM-E4 linker for SGGGSGG and T-K4 linker for $(GGGS)_0$. The data represent means ± standard deviation (n = 3).

improved over those of the PM Q-probe/Fab complex (Table S5A). These results suggest that by examining 12 linker combinations simultaneously, a complex with deeper quenching, which shows a significant fluorescence response against the antigen, can easily be selected.

Application to anti-hapten antibodies

Because Q-body and PM Q-probe/antibody complexes have successfully detected a variety of small molecules,[2,4,7,8,15–20] we applied the CQ-probe to several anti-hapten IgGs, including one anti-CS IgG purified from a hybridoma in our lab (Fig. S2B)[13] and two commercially available antibodies: an anti-testosterone (TS) and an anti-digoxin antibody (Fig. 3A). First, we examined the quenching levels using 12 CQ-probe combinations against these antibodies (Table S3B-D). Similar to the CQ-probe/anti-BGP Fab complex, the fluorescence intensity of the complex tended to decrease in PM-E4 variants with longer linkers, whereas the length of the T-K4 linker did not show any trend. As the base of the PM-E4 linker is located at the C-terminus of the PM, a longer linker would increase the overall mobility of E4 and Dye-K4, and the fluorescent dye in the CQ-probe would easily reach the antigen binding site. In contrast, the T-K4 linker probably controls only the local mobility of the fluorescent dye, and the optimal linker depends on the position of the Trp residue. Next, we selected several complexes out of the 12 combinations with lower fluorescence intensities and examined the fluorescence response upon the addition of the antigen. All CQ-probe/IgG complexes showed a fluorescence response to the antigen; however, the fluorescence response of some complexes was small, and fluorescence recovery from quenching was not sufficient (Table S4B–D and Fig. S3). Therefore, instead of selecting only the deepest quenching combination for optimal linker screening, multiple deep-quenching combinations should be selected and confirmed by antigen addition. When the antigens were added to the best combination of these complexes, the fluorescence intensity increased in a dose-dependent manner (Fig. 3B–D). When we compared the best fluorescence response of the CQ-probe with the control PM Q-probe, we found that the response of complexes with the CQ-probe was higher than that of complexes with the PM Q-probe for anti-CS IgG and anti-digoxin IgG (Fig. 3B, D, and Table S5B). In contrast, the response of the CQ-probe/anti-TS IgG complex was comparable to that of the PM Q-probe (Fig. 3C and Table S5C). These results suggest that the response of complexes with anti-CS IgG or anti-digoxin IgG could be improved by optimization of the linkers between IgG and the fluorescent dye, which allowed the fluorescent dye to be located in the vicinity of both the Trp residues and the antigen binding site. The relatively small improvement of the fluorescence response of complexes with anti-TS IgG can be ascribed to the fluorescent dye of the PM Q-probe being located very close to the optimal position for quenching and fluorescence response. The LOD values of the CQ-probe/antibody complexes were improved over those of the PM Q-probe/antibody complexes for both anti-CS and anti-TS IgG (Table S5B and C). Hence, the improved fluorescence response achieved by employing diverse combinations of CQ-probes extends beyond the scope of a model antibody to encompass multiple anti-hapten IgGs. This approach has the potential for broad applicability to a wide range of antibodies.

Application of R6G-modified K4 peptide for better fluorescence response

The fluorescence response of the Q-body also depends on the compatibility between the fluorescent dye and antibody, and in some cases, Q-bodies with R6G have shown stronger responses to several antibodies than those with TAMRA.[21–23] To obtain a complex with a higher fluorescence response, we examined a CQ-probe containing R6G-K4 (R-K4) (Fig. S1B), which is a K4 peptide modified with R6G instead of TAMRA. This takes advantage of the fact that only fluorescent dye-modified K4 peptides must be prepared. Similar to the CQ-probes using T-K4, we examined the quenching levels using 12 combinations of CQ-probes containing R-K4 for all four antibodies (Table S6). The quenching level trends in the 12 combinations of the complexes with R-K4 were similar to those of the complexes with T-K4 (Table S7, and Fig. S4). This suggests that the high overall mobilities of E4 and Dye-K4 are important, regardless of the structure of the fluorescent dye. We then selected several combinations with deeper quenching and examined their fluorescence responses against the antigens. We obtained the complexes with the best combination and found that their fluorescence responses increased in a dose-dependent manner (Fig. 4). As expected, the response of these complexes to R-K4 was higher than that to T-K4, except for the complex with anti-TS IgG (Table S5). The better fluorescence response using R6G is attributed to the higher hydrophobicity of R6G (lipophilicity index (LogP): 3.4) than that of TAMRA (LogP: 2.9),[24] resulting in deeper quenching by strong interactions with Trp residues. The interaction involves not only hydrophobicity but also other properties such as the orientation and structure of the fluorescent dye, which may not result in a better fluorescence response for some antibodies.[7] On the other hand, the response of the CQ-probe/anti-BGP Fab complex is much larger than that of the PM Q-probe with either TAMRA or R6G. The smaller response observed in the PM Q-probe/anti-BGP Fab complex may come from the excessive flexibility of the linker between PM Q-probe and dye, which does not contain a rigid coiled-coil sequence in the middle. The dye of PM Q-probe is probably more accessible to four Trp residues with a moderate or low contribution to quenching than one Trp residue with a high contribution to quenching (Fig. S5).[4] The LOD values of the complexes with anti-BGP, anti-TS, and anti-digoxin were slightly improved, while that of the complex with anti-CS IgG was not, despite a better fluorescence response. Considering that the value of EC_{50} reflecting antigen-dependent release of fluorescent dye is 50 times higher for the complex using R-K4 than that of T-K4, the strong interaction between R6G and hydrophobic amino acids, such as Trp, in anti-CS IgG required more antigens to release the fluorescent dye for dequenching, leading to reduced sensitivity. Taken together, these results suggest that the CQ-probe with R-K4 is useful for converting antibodies into highly responsive biosensors. Furthermore, by leveraging the easily modified K4 peptide exchange, the CQ-probe is expected to allow for the simultaneous exploration of many linkers with different lengths and sequences, as well as complexes with many different fluorescent dyes.

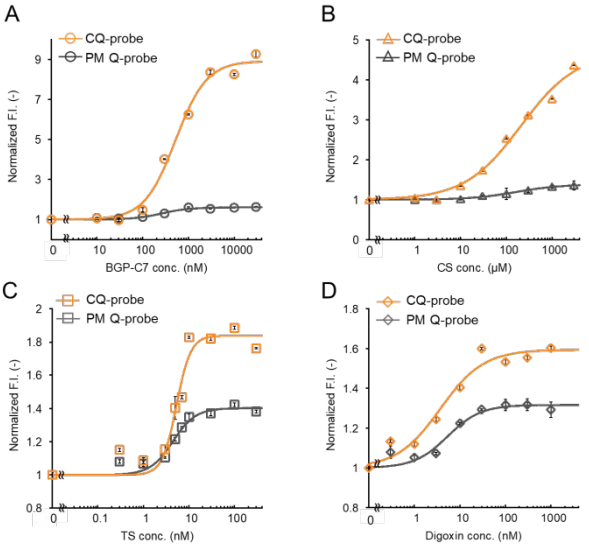

Fig. 4 Dose–response curve of R-K4 labeled CQ-probe/antibody complex against antigens. (A) CQ-probe (1.0 nM)/Fab (30 nM) and PM Q-probe (1.0 nM)/Fab (30 nM) complexes against BGP-C7. The linker combination was the PM-E4 linker for SGGGSMA and the R-K4 linker for $(GGGS)_2$. (B) CQ-probe (1.0 nM)/IgG (5.0 nM) and PM Q-probe (1.0 nM)/IgG (5.0 nM) complexes against cortisol. Linker combinations: PM-E4 linker for SGGGSGG and R-K4 linker for $(GGGS)_2$. (C) CQ-probe (1.0 nM)/IgG (5.0 nM) and PM Q-probe (1.0 nM)/IgG (5.0 nM) complexes against testosterone. Linker combinations: PM-E4 linker for SGGGSMA and R-K4 linker for $(GGGS)_1$. (D) CQ-probe (1.0 nM)/IgG (10 nM) and PM Q-probe (1.0 nM)/IgG (10 nM) complexes against digoxin. Linker combinations: PM-E4 linker for SGGGSGG and R-K4 linker for $(GGGS)_0$. The data represent means ± standard deviation (n = 3).

Conclusions

Here, we developed a fluorescent probe, the CQ-probe, which rapidly optimizes linkers using the strong heterodimer formation of the E4/K4 peptide pair. CQ-probe variants can rapidly screen many linkers simultaneously, allowing for a rapid development process to localize the fluorescent dye of the probe at the optimal position for the fluorescence response. Hence, when complexed with the PM Q-probe, antibodies showing an insufficient fluorescence response to the antigen can be converted into biosensors with a high response using CQ-probe variants. Furthermore, we achieved further response improvements with the CQ-probe using R-K4 instead of T-K4, leading to the generation of a biosensor with improved LOD in some cases. Specifically, an anti-digoxin IgG complex with a CQ-probe using R-K4 was sensitive enough to be used for therapeutic drug monitoring (drug monitoring range: 0.64–1.2 nM) during the treatment of heart failure and arrhythmia.[25]

The anticipated advancements in CQ-probe technology show promise for transforming diverse antibodies into high-performance biosensors with a wide range of applications in clinical diagnosis, environmental surveys, food analysis, and

This journal is © The Royal Society of Chemistry 20xx

biological research. Q-body was shown to be extendable to other fluorescent dyes such as Rhodamine-red, ATTO520, BODIPY-FL, and more, it is likely that CQ-probe is also extendable to the variety of dyes.[21,26] In addition, since Q-body successfully imaged HER2-positive cancer cells without washing steps, CQ-probe is probably applied to imaging as well.[27] In further development, the application of CQ-probes in FACS for targeted cell isolation can be explored.

The PM labeling method, which employs E4/K4 peptides, is an innovative and versatile approach that extends beyond sensor development. It is expected to facilitate modifications not only for fluorescent dyes but also for a diverse array of molecules, such as druggable enzymes and chemical compounds. This convenient technique has greatly improved molecular labeling and broadened the possibilities for molecular research and biomedical applications.

Author contributions

K.S. performed the experiments. T.Y., B.Z., and T.K. advised about the experiments. H.U. conceived the study. H.U. and T.K. designed the experiments. K.S. and T.K. wrote the manuscript. B.Z. and T.Y. edited the manuscript. All authors approved the final version of the manuscript.

Conflicts of interest

T.Y., B.Z., H.U., and T.K. received honoraria from HikariQ Health, Inc. for another project.

Acknowledgments

We thank Norihiko Kobayashi at Kobe Pharmaceutical University for providing the CS#4-6 hybridoma cells that produced the mouse anti-CS monoclonal antibody. This work was supported by a Japan Society for the Promotion of Science (JSPS) Grant-in-Aid for Scientific Research (KAKENHI) (JP22H05176 to T.K.), Japan Science and Technology Agency (JST) SPRING (JPMJSP2106 to K.S.), a Research Grant from the Nakatani Foundation (to H.U. and T.K.), and the Mishima Kaiun Memorial Foundation (to T.K.).

References

1 R. K. Grover, X. Zhu, T. Nieusma, T. Jones, I. Boreo, A. S. MacLeod, A. Mark, S. Niessen, H. J. Kim, L. Kong, N. A. Assad-Garcia, K. Kwon, M. Chesi, V. V. Smider, D. R. Salomon, D. F. Jelinek, R. A. Kyle, R. B. Pyles, J. I. Glass, A. B. Ward, I. A. Wilson and R. A. Lerner, *Science*, 2014, **343**, 656–661.
2 J. Dong, C. Miyake, T. Yasuda, H. Oyama, I. Morita, T. Tsukahara, M. Takahashi, H. J. Jeong, T. Kitaguchi, N. Kobayashi and H. Ueda, *Biosens. Bioelectron.*, 2020, **165**, 112425.
3 N. Marmé, J. P. Knemeyer, M. Sauer and J. Wolfrum, Bioconjugate Chem., 2003, 14, 1133–1139.
4 R. Abe, H. Ohashi, I. Iijima, M. Ihara, H. Takagi, T. Hohsaka and H. Ueda, *J. Am. Chem. Soc.*, 2011, **133**, 17386–17394.
5 H. Ohashi, T. Matsumoto, H. Jeong, J. Dong, R. Abe and H. Ueda, *Bioconjug. Chem.*, 2016, **27**, 2248–2253.
6 R. Takahashi, T. Yasuda, Y. Ohmuro-Matsuyama and H. Ueda, *Anal. Chem.*, 2021, **93**, 7571–7578.
7 A. Inoue, Y. Ohmuro-Matsuyama, T. Kitaguchi and H. Ueda, *ACS Sens.*, 2020, **5**, 3457–3464.
8 A. Sasao, M. Takaki, H. J. Jeong, K. Yonemitsu, Y. Ohtsu, H. Tsutsumi, S. Furukawa, H. Morioka, H. Ueda and Y. Nishitani, *Drug Test. Anal.*, 2019, **11**, 601–609.
9 J. R. Litowski and R. S. Hodges, *J. Biol. Chem.*, 2002, **277**, 37272–37279.
10 Y. Yano, A. Yano, S. Oishi, Y. Sugimoto, G. Tsujimoto, N. Fujii and K. Matsuzaki, *ACS Chem. Biol.*, 2008, **3**, 341–345.
11 T. Yasuda, A. Inoue, T. Kitaguchi and H. Ueda, *Chem. Commun. (Camb)*, 2021, **57**, 8206–8209.
12 J. Dong, H. J. Jeong and H. Ueda, *J. Biosci. Bioeng.*, 2016, **122**, 125–130.
13 H. Oyama, I. Morita, Y. Kiguchi, S. Miyake, A. Moriuchi, T. Akisada, T. Niwa and N. Kobayashi, *Anal. Chem.*, 2015, **87**, 12387–12395.
14 S. L. Lim, H. Ichinose, T. Shinoda and H. Ueda, *Anal. Chem.*, 2007, **79**, 6193–6200.
15 R. Abe, H. J. Jeong, D. Arakawa, J. H. Dong, H. Ohashi, R. Kaigome, F. Saiki, K. Yamane, H. Takagi and H. Ueda, *Sci. Rep.*, 2014, **4**, 4640.
16 S. Zhao, R. Zhang, Y. Gao, Y. Cheng, S. Zhao, M. Li, H. Li and J. Dong, *ACS Omega*, 2023, **8**, 15341–15349.
17 J. Liang, H. Dong, H. Wang, Z. Yi, G. Jiang, T. Inagaki, C. E. Gomez-Sanchez, J. Dong and H. Ueda, *J. Steroid Biochem. Mol. Biol.*, 2022, **221**, 106118.
18 J. Dong, H. Xu, F. Li, B. Li, H. Chen, L. Li, M. Liu, Y. Jiang and G. Dong, *Front. Bioeng. Biotechnol.*, 2022, **10**, 818983.
19 H. J. Jeong, J. Dong, C. H. Yeom and H. Ueda, *Methods Protoc.*, 2020, **3**, 43.
20 S. Zhao, J. Dong, H. J. Jeong, K. Okumura and H. Ueda, *Anal. Bioanal. Chem.*, 2018, **410**, 4219–4226.
21 H. J. Jeong, T. Kawamura, J. Dong and H. Ueda, *ACS Sens.*, 2016, **1**, 88–94.
22 J. Dong, B. Banwait, H. Ueda and P. Kristensen, *Sensors*, 2023, **23**, 2251.
23 H. J. Jeong, Y. Ohmuro-Matsuyama, H. Ohashi, F. Ohsawa, Y. Tatsu, M. Inagaki and H. Ueda, *Biosens. Bioelectron.*, 2013, **40**, 17–23.
24 M. Ogawa, N. Kosaka, P. L. Choyke and H. Kobayashi, *ACS Chem. Biol.*, 2009, **4**, 535–546.
25 P. A. Heidenreich, B. Bozkurt, D. Aguilar, L. A. Allen, J. J. Byun, M. M. Colvin, A. Deswal, M. H. Drazner, S. M. Dunlay, L. R. Evers, J. C. Fang, S. E. Fedson, G. C. Fonarow, S. S. Hayek, A. F. Hernandez, P. Khazanie, M. M. Kittleson, C. S. Lee, M. S. Link, C. A. Milano, L. C. Nnacheta, A. T. Sandhu, L. W. Stevenson, O. Vardeny, A. R. Vest and C. W. Yancy, *Circulation*, 2022, **145**, e895–e1032.
26 S. Sato, M. Matsumura, H. Ueda and H. Nakamura, *Chem. Commun.*, 2021, **57**, 9760–9763.
27 J. Dong, Y. Oka, H.J. Jeong, Y. Ohmuro-Matsuyama and H. Ueda, *Biotechnol. Bioeng.*, 2020, **117**, 1259–1269.